Supplementary Material (ESI) for Chemical Communications
This journal is © The Royal Society of Chemistry 2013

Boron-pyridyl-imino-isoindoline dyes: facile synthesis and photophysical properties

Hui Liu,[a] Hua Lu,[a,] * Jing Xu,[a] Zhipeng Liu,[d] Zhifang Li,[a] John Mack,[c,] * Zhen Shen[b,] *

I. Experimental section

II. Supplementary Figure

I. Experimental Section

I.1 Materials and instrumentations

All reagents were obtained from commercial suppliers and used without further purification unless otherwise indicated. All air and moisture-sensitive reactions were carried out under nitrogen atmosphere in oven-dried glassware. Glassware was dried in an oven at 100 °C and cooled under a stream of inert gas before use. Both dichloromethane and triethylamine were distilled over calcium hydride. ^{1}H NMR spectra were recorded on a Bruker DRX400 spectrometer and referenced to the residual proton signals of the solvent. HR-MS were recorded on a Bruker Daltonics microTOF-Q II spectrometer. All the solvents employed for the spectroscopic measurements were of UV spectroscopic grade (Aldrich).

I.2 Synthesis and characterisation

Boron-pyridyl-imino-isoindolines (**1**)

A solution of 3-iminoisoindolin-1-one (161 mg, 1.1 mmol) and 2-aminopyridine (104 mg, 1.1 mmol) in ethanol (10 ml) was heated under reflux for 20h, ammonia was evolved, when the solution was cooled, a colorless solid was precipitated. The crude product was dissolved in dry dichloromethane solution (100 ml) and treated with $BF_3 \cdot OEt_2$ (2.2 ml) in the presence of triethylamine (2 ml) at room temperature for 1 h. The reaction was quenched by adding water, the organic layer was dried over $MgSO_4$, filtered, and evaporated to dryness. The crude product was purified by silica-gel flash column chromatography (75% Hexane/Ethyl acetate) and recrystallized from CH_2Cl_2/hexane to provide **1** as colorless crystals (60 mg, 20%). ^{1}H NMR (400 MHz, $CDCl_3$) $\delta = 8.60$ (d, $J = 4.0$ Hz, 1 H), 8.15 (t, $J = 8$ Hz, 1 H), 8.03 (t, $J = 4.8$ Hz, 1 H), 7.94 (t, $J = 3.2$ Hz 1 H), 7.73–7.70 (m, 3 H), 7.48 (t, $J = 6.4$ Hz, 1 H); Uv/Vis (CH_2Cl_2), λ_{max} (ε) = 361 nm (24400 dm^3 mol^{-1} cm^{-1}); HRMS-ESI: m/z: calcd $[C_{13}H_8BF_2N_3ONa]^+$ m/z = 294.0621; found m/z = 294.0622 $[M+Na^+]$, 272.0794, $[M+H^+]$, 252.0718, $[M-F]^+$.

Compound **2** was obtained as yellow crystals in 22% yield by following a procedure similar to that of **1**. ^{1}H NMR (400 MHz, CDCl$_3$): δ = 8.91 (d, *J* = 9.6 Hz, 1 H), 8.45 (d, *J* = 8.8 Hz, 1H), 8.07 (t, *J* = 4.8 Hz, 1 H), 7.98 (d, *J* = 4.8 Hz, 1 H), 7.90 (d, *J* = 7.2 Hz, 2 H), 7.76 (m, 2 H), 7.69 (m, 2 H); Uv/Vis (CH$_2$Cl$_2$), λ_{max} (ε) = 387 nm (26700 dm^3 mol^{-1} cm^{-1}); HRMS-ESI: m/z: calcd [C$_{17}$H$_{10}$BF$_2$N$_3$ONa]$^+$ m/z = 344.0777; found m/z = 344.0782 [M+Na$^+$].

Compound **3** was obtained as a light yellow solid in 18% yield by following a procedure similar to that of **1**. ^{1}H NMR (400 MHz, CDCl$_3$): δ = 8.61 (m, 1 H), 8.55 (s, 1 H), 8.47 (s, 1 H), 8.14 (t, *J* = 7.2 Hz, 1 H), 8.08 (m, *J* = 3.6 Hz, 2 H), 7.71 (t, *J* = 8.0 Hz, 3 H), 7.46 (t, *J* = 7.0 Hz, 1 H); Uv/Vis (CH$_2$Cl$_2$), λ_{max} (ε) = 396 nm (31700 dm^3 mol^{-1} cm^{-1}); HRMS-ESI: m/z: calcd [C$_{17}$H$_{10}$BF$_2$N$_3$ONa]$^+$ m/z = 344.0777; found m/z = 344.0780 [M+Na$^+$], 322.0961, [M+H$^+$].

Compound **4** was obtained as yellow crystals in 19% yield by following a procedure similar to that of **1**. ^{1}H NMR (400 MHz, CDCl$_3$): δ= 8.91 (m, 1 H), 8.61 (s, 1 H), 8.49 (s, 1H), 8.44 (d, *J* = 8.8 Hz, 1 H), 8.10 (m, 2 H), 7.91 (t, *J* = 7.6 Hz, 2 H), 7.65- 7.73 (m, 4 H); Uv/Vis (CH$_2$Cl$_2$), λ_{max} (ε) = 419 nm (47500 dm^3 mol^{-1} cm^{-1}). HRMS-ESI: m/z: calcd [C$_{21}$H$_{12}$BF$_2$N$_3$ONa]$^+$ m/z = 394.0934; found m/z = 394.0954 [M+Na$^+$].

I.3 X-ray structure determination

The X-ray diffraction data were collected on a Bruker Smart Apex CCD diffractometer with graphite monochromated Mo Kα radiation (λ = 0.71073 Å) using the ω−2θ scan mode. The structure was solved by direct methods and refined on F^2 by full-matrix least-squares methods using SHELX-2000.[S1-S2] All calculations and molecular graphics were carried out on a computer using the SHELX-2000 program package and Diamond 3.2.

1: C$_{13}$H$_8$BF$_2$N$_3$O; A colorless block-like crystal of the approximate dimensions 0.22 × 0.20 × 0.20 mm^3 was measured. Monoclinic, space group P2(1)/c, *a* = 7.1416(9) Å, *b* = 8.4969(11) Å, *c* = 19.655(3) Å, α = 90, β = 99.473(2), γ = 90, V = 1176.4(3)

Å^3, Z = 4, F(000) = 552.0, ρ = 1.530 Mgm^{-3}, R_1 = 0.0373, wR_2 = 0.1110, GOF = 1.326, residual electron density between 0.140 and −0.222 eÅ^{-3}.

2: $C_{17}H_{10}BF_2N_3O$; A colorless block-like crystal of the approximate dimensions 0.24 × 0.21 × 0.22 mm^3 was measured. Monoclinic, space group P2(1)/c, *a* = 8.575(2) Å, *b* = 12.611(3) Å, *c* = 13.588(3) Å, α = 90, β = 106.164(4), γ = 90, V = 1411.3(6) Å^3, Z = 4, F(000) = 656.0, ρ = 1.511 Mgm^{-3}, R_1 = 0.0397, wR_2 = 0.1150, GOF = 1.256, residual electron density between 0.146 and −0.250 eÅ^{-3}.

4: $C_{21}H_{12}BF_2N_3O$: A yellow block-like crystal of the approximate dimensions 0.26 × 0.20 × 0.18 mm^3 was measured. Monoclinic, space group P2(1)/c, *a* = 15.707(17) Å, *b* = 15.0371(16) Å, *c* = 16.4939(18) Å, α = 90, β = 112.855(2), γ = 90, V = 3589.8(7) Å^3, Z = 4, F(000) = 1688.0, ρ = 1.531 Mgm^{-3}, R_1 = 0.0420, wR_2 = 0.1221, GOF = 1.020, residual electron density between 0.521 and −0.562 eÅ^{-3}.

CCDC No. 968011 for **1**, No. 968012 for **2** and No 968013 for **4** containing the supplementary crystallographic data for this paper. These data can be obtained free of charge via www.ccdc.cam.ac.uk/conts/retrieving.html (or from the Cambridge Crystallographic Data Centre, 12 Union Road, Cambridge CB21EZ, UK; fax: (+44)1223–336–033; E-mail: deposit@ccdc.cam.ac.uk).

1.4 Spectroscopic measurements

UV-visible absorption spectra were recorded on a Shimadzu 3000 spectrophotometer. Fluorescence spectra were measured on a Hitachi F-2700 luminescence spectrometer with a 150 W xenon lamp. The fluorescence lifetimes and the absolute quantum yields (Φ_F) of the samples were determined with a Horiba Jobin Yvon Fluorolog-3 spectrofluorimeter. Absorption and emission measurements were carried out in 1×1 cm quartz cuvettes. Drop casting films were prepared by evaporation of the dye (1 mM) in dichloromethane onto a clean silicon wafer substrates, then the absorption spectras were measured in Shimadzu 3000 spectrophotometer by a general method. The absolute quantum yields and emission spectra in the solid state were measured in

Horiba Jobin Yvon Fluorolog-3 spectrofluorimeter with integrating sphere. Those films were stable and no change in absorption and emission was observed over an extended period of time. For all measurements, the temperature was kept constant at (298±2) K. Dilute solutions with absorbance of less than 0.05 at the excitation wavelength were used for the measurement of fluorescence quantum yields. 9,10-Diphenylanthracene was used as the standard (Φ_F = 0.90 in cyclohexane).[S3] The quantum yield, Φ, was calculated using equation (1):

$$\Phi_{sample}=\Phi_{std}\left[\frac{I\ sample}{I\ std}\right]\left[\frac{A\ std}{A\ sample}\right]\left[\frac{n2\ sample}{n2\ std}\right] \quad (1)$$

where the *sample* and *std* subscripts denote the sample and standard, respectively, *I* is the integrated emission intensity, *A* stands for the absorbance, and *n* is refractive index.

When the fluorescence decays were monoexponential, the rate constants of radiative (k_f) and nonradiative (k_nr) deactivation were calculated from the measured fluorescence quantum yield (Φ_F) and fluorescence lifetime (τ) according to equations (2) and (3):

$$k_\mathrm{f} = \Phi_F/\tau \quad (2)$$

$$k_\mathrm{nr} = (1-\Phi_F)/\tau \quad (3)$$

I.5 DFT calculations

The G09W software package was used to carry out a DFT geometry optimization using the CAM-B3LYP functional with 6-31G(d) basis sets.[S4] The same approach was used to calculate the absorption properties based on time-dependent (TD-DFT) method.

II Supplementary data

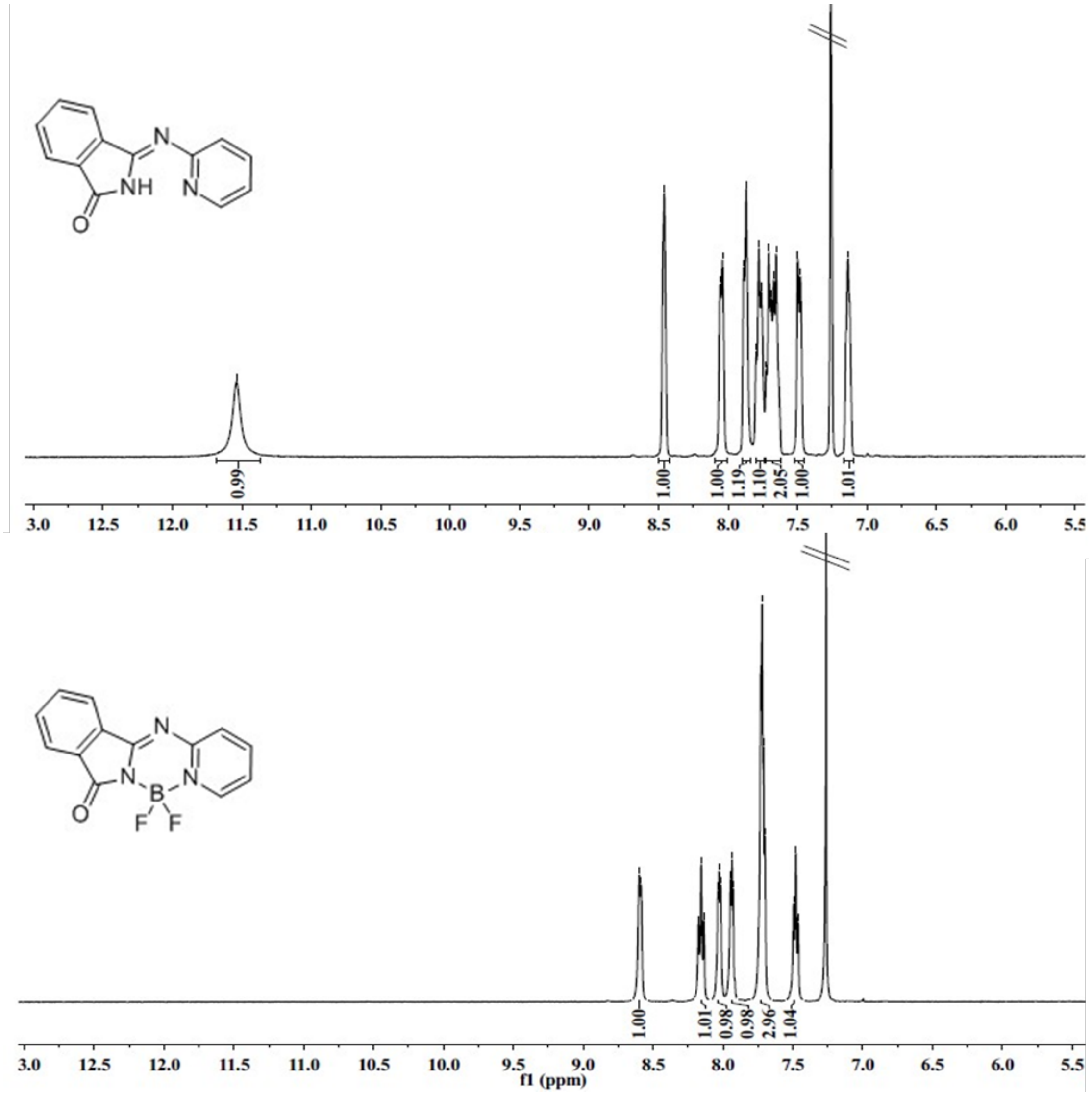

Fig. S1 ^{1}H NMR spectra of **1** and it's precursor Keto-pyridyliminoisoindoline.

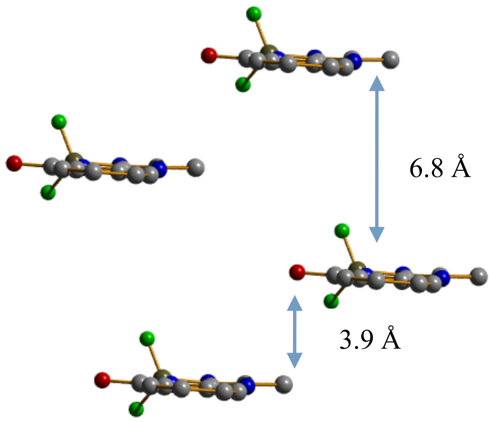

1

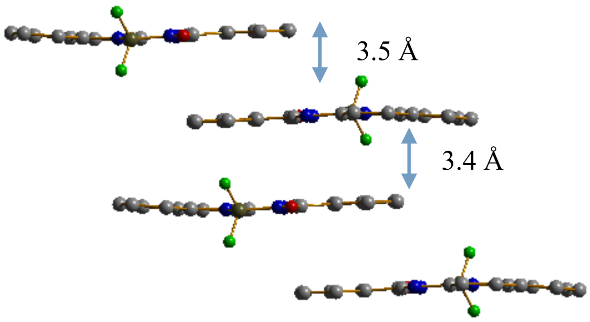

2

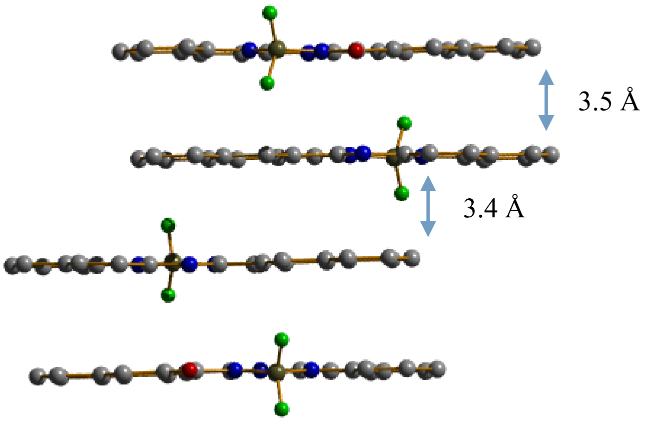

4

Fig. S2 View of the π–π stacking interactions of **1**, **2** and **4.**

Table S1. Spectroscopic and photophysical properties of **1-4** in various solvents at 298K.

	Solvent	λ_{abs} [nm]	ε_{abs}[a]	λ_{em} [nm]	$\Delta\nu_{em\text{-}abs}$ [nm]	Φ_F	τ_f [ns]	k_r [10^8 s^{-1}]	k_{nr} [10^8 s^{-1}]
1	hexane	359, 377(sh)	21300	384(sh), 406	7	0.05	<0.20	nd	nd
	Toluene	363, 380(sh)	22800	395(sh), 417	15	0.32	0.90	3.55	7.55
	CH_2Cl_2	361, 379(sh)	24400	391(sh), 413	12	0.33	1.01	3.27	6.63
	THF	361, 378(sh)	23300	390(sh), 414	12	0.18	0.64	2.81	12.8
	CH_3CN	360, 378(sh)	22600	391(sh), 413	13	0.15	0.58	2.59	14.65
2	hexane	384, 403(sh)	nd	410(sh), 436	12	0.45	1.53	2.94	3.59
	Toluene	388, 407(sh)	34100	418(sh), 443	11	0.89	2.76	3.22	0.40
	CH_2Cl_2	387, 406(sh)	26700	417(sh), 444	11	0.74	2.54	2.91	0.10
	THF	386,404(sh)	35800	415(sh), 442	11	0.73	2.27	3.22	1.19
	CH_3CN	384, 403(sh)	32600	417(sh), 442	14	0.85	2.52	3.37	0.60
3	hexane	389	nd	396	7	0.55	0.98	5.61	4.59
	Toluene	396	34500	409	13	0.79	2.41	3.27	0.87
	CH_2Cl_2	396	31700	414	18	0.86	2.25	3.82	0.62
	THF	393	34100	409	16	0.85	2.32	3.66	0.65
	CH_3CN	393	30500	425	32	0.96	3.00	3.20	0.13
4	hexane	413	nd	419	6	0.63	1.79	3.52	2.07
	Toluene	419	48300	427	8	0.79	1.64	4.82	1.28
	CH_2Cl_2	419	47500	430	11	0.90	1.93	4.66	0.52
	THF	416	43350	425	9	0.76	1.68	4.52	1.43
	CH_3CN	416	42050	434(sh), 451	18	0.81	2.09	3.88	0.91

[a] The molar absorption coefficient was measured in solution containing 1% CH_2Cl_2 as a co-solvent. nd= not determined, sh=shoulder

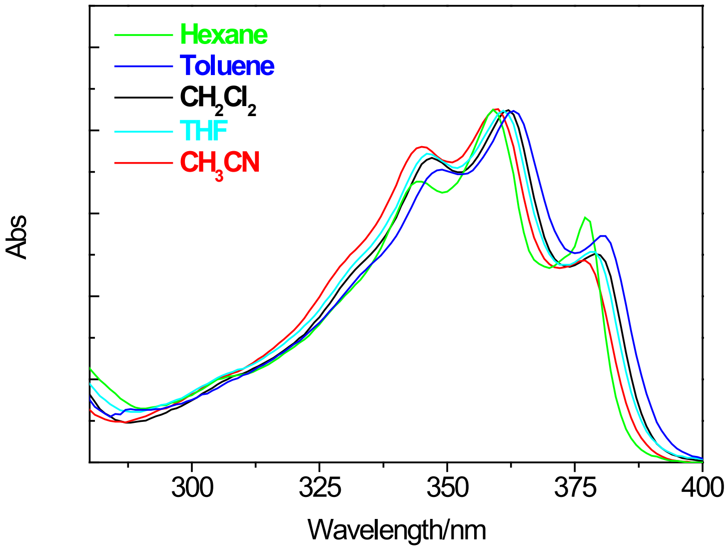

Fig. S3. Absorption spectra of **1** in a range of different solvents.

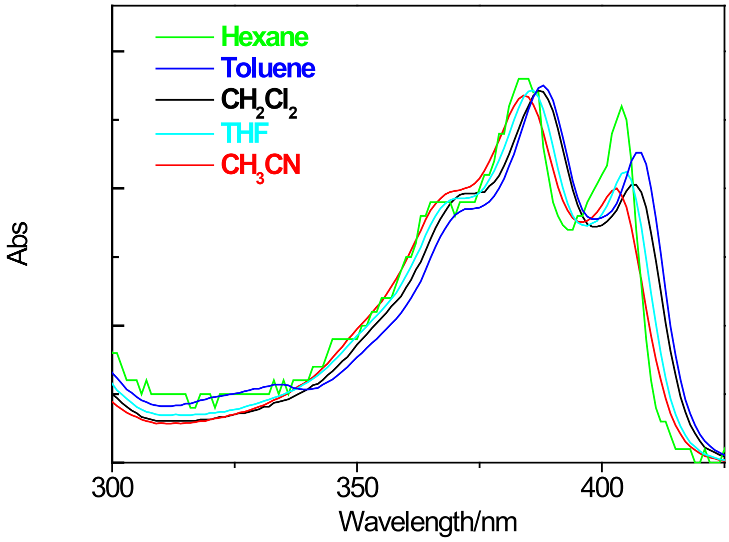

Fig. S4. Absorption spectra of **2** in a range of different solvents.

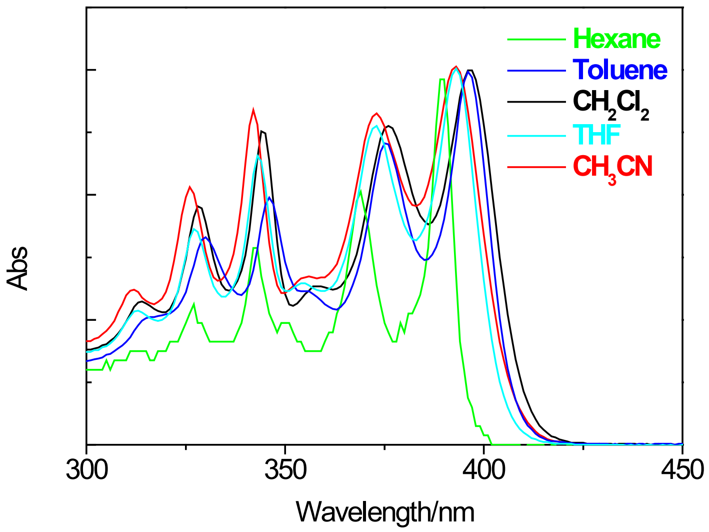

Fig. S5. Absorption spectra of **3** in a range of different solvents.

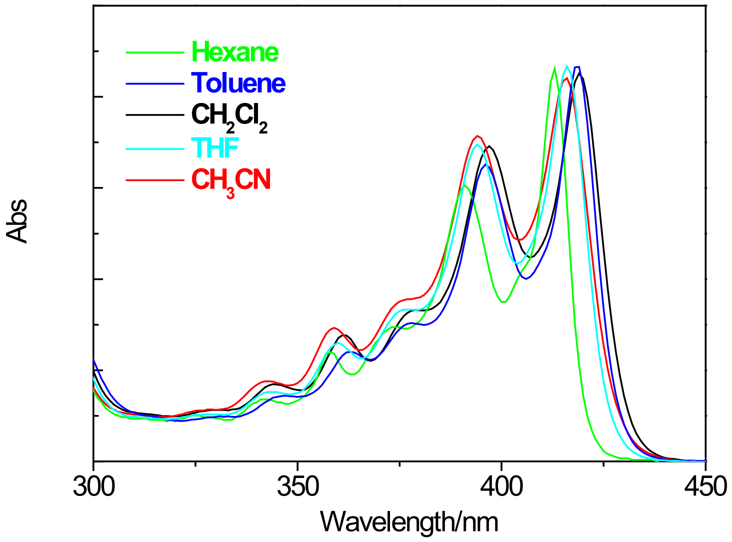

Fig. S6. Absorption spectra of **4** in a range of different solvents.

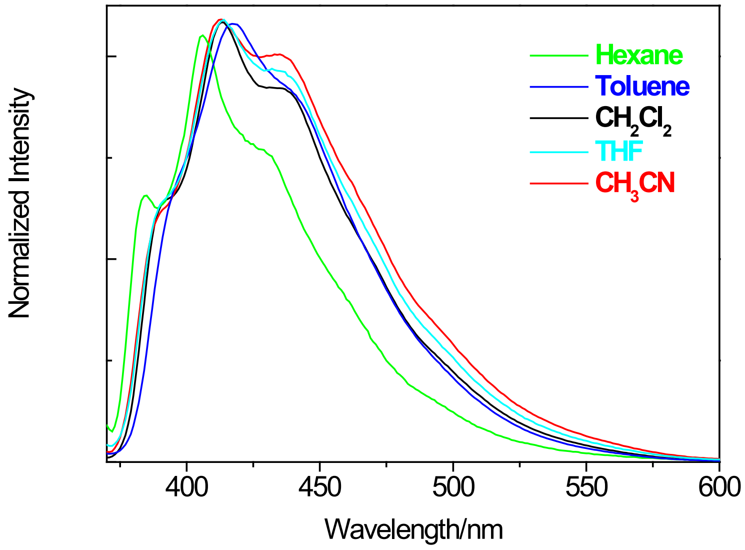

Fig. S7. Emission spectra of **1** in a range of different solvents.

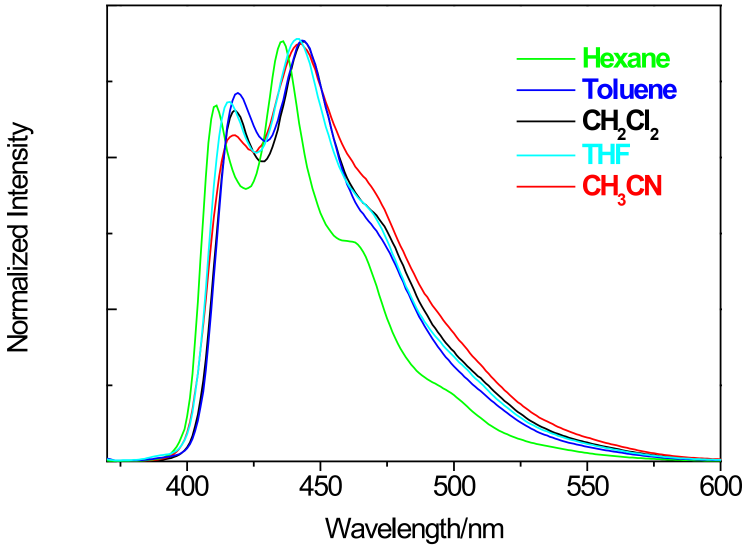

Fig. S8. Emission spectra of **2** in a range of different solvents.

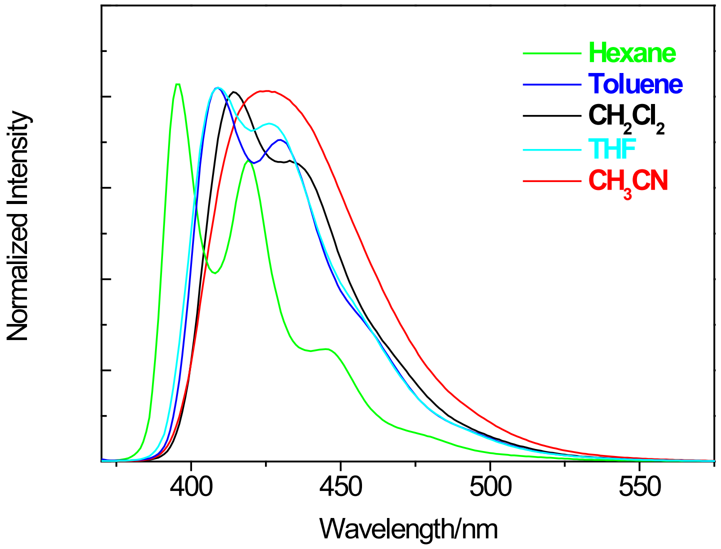

Fig. S9. Emission spectra of **3** in a range of different solvents.

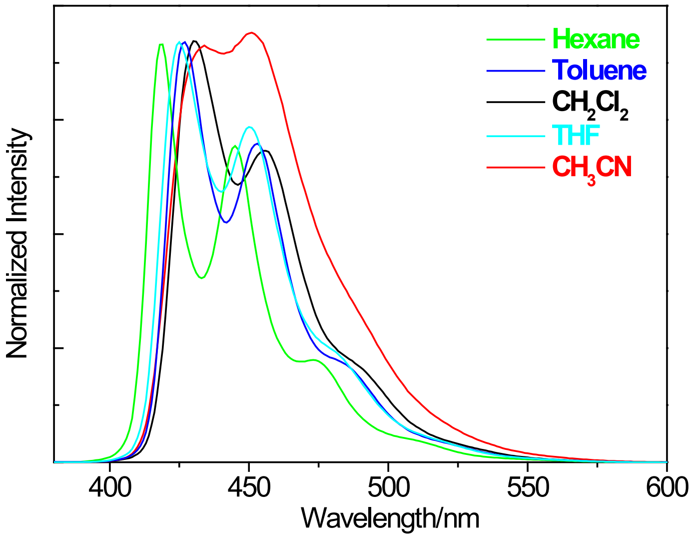

Fig. S10. Emission spectra of **4** in a range of different solvents.

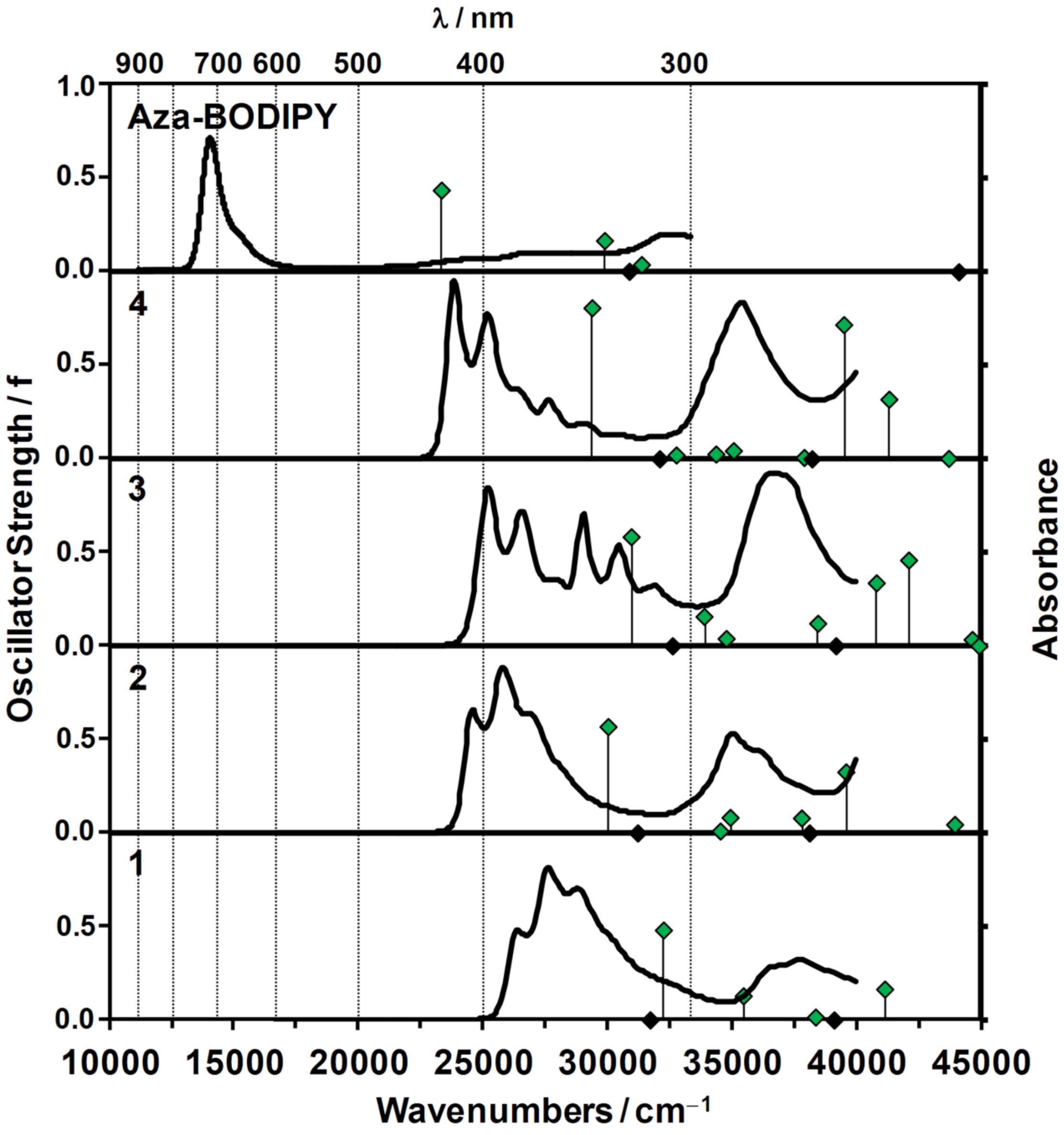

Fig. S11 TD-DFT spectra of **1-4** and aza-BODIPY calculated using the CAM-B3LYP functional with 6-31G(d) basis sets. Green and black diamonds denote ππ* and σπ* transitions, respectively. The experimental spectra **1-4** and aza-BODIPY[S5] are plotted against a secondary axis.

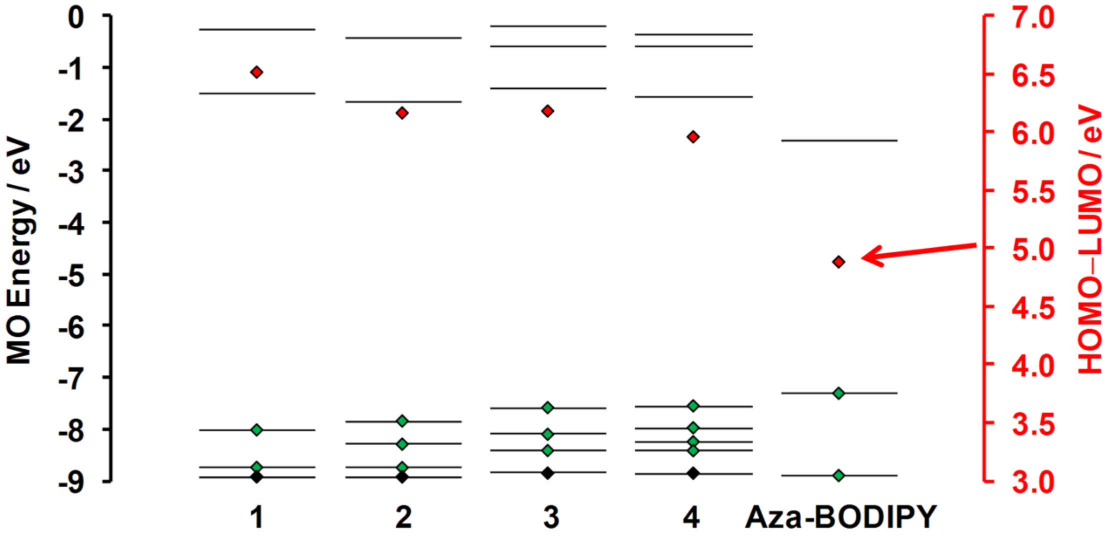

Fig. S12. MO energies for aza-BODIPY and **1-4** in the TD-DFT calculations carried out using the CAM-B3LYP functional with 6-31G(d) basis sets. Green and black diamonds denote occupied π-MOs and σ-MOs, respectively. The predicted HOMO–LUMO band gaps are plotted against a secondary axis.

Table S2. Calculated electronic excitation energies, oscillator strengths, and eigenvectors for the TD-DFT spectra of **1-4** and aza-BODIPY (**5**) carried out using the CAM-B3LYP functional with 6-31G(d) basis sets.

	State[a]	Energy[eV]	λ [nm]	f[b]	Eigenvectors[c]	Band[d]
1	S_1	3.95	315	0.0008	H−3 → L(78%)	σπ*
	S_2	4.01	310	0.4812	H → L(84%)	ππ*
	S_3	4.41	282	0.1295	H−1 → L(79%)	ππ*
	S_4	4.77	261	0.016	H−2 → L(64%); H−1 → L+2(13%)	ππ*
	S_5	4.87	256	0.0004	H−4 → L(87%)	σπ*
2	S_1	3.74	333	0.5688	H → L(94%)	ππ*
	S_2	3.88	321	0.0003	H−3 → L(78%); H−3 → L+1(10%)	σπ*
	S_3	4.30	290	0.0104	H−2 → L(42%); H−1 → L(40%)	ππ*
	S_4	4.35	286	0.0831	H−2 → L(39%); H−1 → L(41%)	ππ*
	S_5	4.70	265	0.08	H−4 → L(58%); H → L+1(12%); H−2 → L+2(10%)	ππ*
	S_6	4.74	262	0.0001	H−6 → L(87%)	σπ*
	S_7	4.93	253	0.3265	H → L+1(37%); H−1 → L+1(12%); H−5 → L(11%); H−4 → L(10%)	ππ*
3	S_1	3.85	323	0.5836	H → L(81%)	ππ*
	S_2	4.06	308	0.0004	H−3 → L(74%); H−3 → L+1(11%)	σπ*
	S_3	4.22	295	0.1575	H−1 → L(62%); H−2 → L+1(16%)	ππ*
	S_4	4.33	288	0.0397	H−2 → L(51%); H → L+1(33%)	ππ*
	S_5	4.78	260	0.1209	H → L+1(52%); H−2 → L(26%)	ππ*
	S_6	4.88	255	0.0008	H−5 → L(76%)	σπ*
4	S_1	3.66	340	0.8075	H → L(79%); H−1 → L(11%)	ππ*
	S_2	3.99	312	0.0002	H−4 → L(72%)	σπ*
	S_3	4.08	305	0.0207	H−1 → L(58%); H−3 → L+1(16%); H−1 → L+2(11%)	ππ*
	S_4	4.28	291	0.0258	H−3 → L(50%); H → L+1(21%)	ππ*
	S_5	4.36	285	0.0439	H−2 → L(70%)	ππ*
	S_6	4.72	264	0.0074	H → L+1(46%); H−3 → L(15%); H−1 → L+1(11%)	ππ*
	S_7	4.76	262	0.0001	H−6 → L(78%)	σπ*
	S_8	4.91	253	0.7175	H → L+2(19%); H−1 → L+2(19%); H−2 → L+2(10%)	ππ*
5	S_1	2.90	429	0.4366	H → L(92%)	ππ*
	S_2	3.72	335	0.1671	H−1 → L(91%)	ππ*
	S_3	3.84	324	0.0026	H−3 → L(98%)	σπ*
	S_4	3.90	319	0.0388	H−2 → L(99%)	ππ*

[a] Excited state. [b] Oscillator strength. [c] MOs involved in the transitions with H and L denoting the HOMO and LUMO, respectively. [d] Type of excited state.

III. References

S1 C. L. Picou, E. D. Stevens, M. Shah and J. H. Boyer, *Acta Crystallogr. Sect. C* 1990, **46**, 1148.

S2 SMART, SAINT, SADABS and SHELXTL, Bruker AXS Inc., Madison, 2000.

S3 S. Hamai and F. Hirayama, *J. Phys. Chem.*, 1983; **87**, 83-89.

S4 Gaussian 09, Revision D.01, M. J. Frisch, G. W. Trucks, H. B. Schlegel, G. E. Scuseria, M. A. Robb, J. R. Cheeseman, G. Scalmani, V. Barone, B. Mennucci, G. A. Petersson, H. Nakatsuji, M. Caricato, X. Li, H. P. Hratchian, A. F. Izmaylov, J. Bloino, G. Zheng, J. L. Sonnenberg, M. Hada, M. Ehara, K. Toyota, R. Fukuda, J. Hasegawa, M. Ishida, T. Nakajima, Y. Honda, O. Kitao, H. Nakai, T. Vreven, J. A. Montgomery, Jr., J. E. Peralta, F. Ogliaro, M. Bearpark, J. J. Heyd, E. Brothers, K. N. Kudin, V. N. Staroverov, R. Kobayashi, J. Normand, K. Raghavachari, A. Rendell, J. C. Burant, S. S. Iyengar, J. Tomasi, M. Cossi, N. Rega, J. M. Millam, M. Klene, J. E. Knox, J. B. Cross, V. Bakken, C. Adamo, J. Jaramillo, R. Gomperts, R. E. Stratmann, O. Yazyev, A. J. Austin, R. Cammi, C. Pomelli, J. W. Ochterski, R. L. Martin, K. Morokuma, V. G. Zakrzewski, G. A. Voth, P. Salvador, J. J. Dannenberg, S. Dapprich, A. D. Daniels, Ö. Farkas, J. B. Foresman, J. V. Ortiz, J. Cioslowski, and D. J. Fox, Gaussian, Inc., Wallingford CT, 2009.

S5 H. Lu, S. Shimizu, J. Mack, X. Z. You, Z. Shen. N. Kobayashi, *Chem. Asian J.*, 2011, **6**, 1026–1037.